Rendering Participating Media with Bidirectional Path Tracing

Eric P. Lafortune and Yves D. Willems

Paper presented at the 7th Eurographics Workshop on Rendering

Please send any correspondence to:
Eric Lafortune
Cornell University
Program of Computer Graphics
580 Rhodes Hall
Ithaca, NY 14853-3801
Telephone: +1 - 607 - 255 - 4880
Fax: +1 - 607 - 255 - 0806
E-mail: Eric.Lafortune@cs.kuleuven.ac.be

Rendering Participating Media with Bidirectional Path Tracing

Eric P. Lafortune and Yves D. Willems

Department of Computer Science, Katholieke Universiteit Leuven
Celestijnenlaan 200A, 3001 Heverlee, Belgium
Eric.Lafortune@cs.kuleuven.ac.be

Abstract: In this paper we show how bidirectional path tracing can be extended to handle global illumination effects due to participating media. The resulting image-based algorithm is computationally expensive but more versatile than previous solutions. It correctly handles multiple scattering in non-homogeneous, anisotropic media in complex illumination situations. We illustrate its specific advantages by means of examples.

1 Introduction

Most current global illumination algorithms ignore the influence of the medium through which the light travels. In these illumination simulations, light is only emitted and reflected at surfaces; the absorption, scattering and emission of light as a result of smoke, dust, fog or flames are neglected. While this is a reasonable approximation for most daily scenes, the presence of media can sometimes enhance the realistic appearance of renderings. A typical example is the beam of light from the sun shining through a window of a dusty interior. In other applications such as visibility studies for traffic or for fire exits in buildings, the medium even plays a central role in the simulation problem.

Rushmeier [1] and others [2, 3] have presented extensive overviews of research efforts and packages for the simulation of light in participating media. Depending on the applications they handle homogeneous or non-homogeneous and isotropic or anisotropic media. Many techniques only model single scattering, which suffices for optically thin media. Most approaches can be classified into a few basic categories: zonal methods for isotropic scattering, P_N methods, discrete ordinate methods, point collocation methods and image-based Monte Carlo methods. A zonal method that handles participating media was presented by Rushmeier [4], as an extension to the basic radiosity algorithm. The algorithm assumes that the participating medium is isotropic and computes the exchange of light between the discretised volume elements and the surface elements in the scene. P_N methods also discretise the volume into finite elements, but now represent the radiance function as a series of spherical harmonics. They then solve the problem in its differential form, e.g. [5, 6]. Discrete ordinate methods discretise not only the original volume into finite volume elements, but also the directions of the sphere into finite solid angles, e.g. [7]. This lifts the assumption of the zonal methods that the participating medium is isotropic, at the cost of increased memory requirements. Languénou *et al.* [2] and Max [3] present algorithms to efficiently distribute power between the discrete elements. Point collocation methods use higher order basis functions, such as spherical harmonics, to represent the illumination function over the sphere, e.g. [8].

Monte Carlo methods are generally either an extension to the path tracing algorithm as proposed by Kajiya [9] or to light tracing algorithms, as pioneered by Arvo [10]. Rushmeier [4] for instance presents an extension to the path tracing algorithm. It traces random walks starting from the eye point, reflecting at surfaces and additionally scattering in the medium. Roysam *et al.* [11] and Rozé *et al.* [12] apply light tracing approaches, tracing random walks from the light sources, until they hit a detector. Pattanaik [13] follows this approach in the context of a zonal method, updating the radiosity values at discrete volume and surface elements.

In this contribution we propose an image-based Monte Carlo solution, now applying bidirectional path tracing rather than just path tracing. The approach thus integrates previous light shooting and light gathering techniques for participating media. Section 2 recalls the mathematical model of global illumination for scenes with a participating medium. We discuss the case of non-emitting media with possibly anisotropic scattering, starting with homogeneous media. Section 3 explains how a random walk through the scene can be sampled on the basis of the mathematical framework. Section 4 then shows how these random walks integrate in the bidirectional path tracing algorithm. This image-based approach is very general, like path tracing, but better suited to handle complex illumination situations. Section 5 shows how the handling of homogeneous media can be further extended to non-homogeneous media. Section 6 presents some results to demonstrate the versatility of the algorithms. We indicate specific advantages and disadvantages of the algorithm and draw some final conclusions in section 7.

2 Mathematical model

In its most commonly used form, the rendering equation defines the radiance function, assuming that it is invariant along the direction in which it is radiated. The equation can be extended fairly easily to account for participating media. In this case radiance changes gradually along a line, as light is absorbed, outscattered to other directions and inscattered from other directions. The integral equation defining the radiance function inside the medium becomes an integro-differential equation:

$$\frac{\partial L(x,\Theta)}{\partial s} = \sigma(x) \int_{\Omega} f(x,\Theta',\Theta) L(x,\Theta') d\omega' - \kappa(x) L(x,\Theta) \tag{1}$$

where:

- x is a point in the 3D space,
- Θ is a direction,
- ds is a differential distance along direction Θ $[m]$,
- Ω is the sphere of directions,
- $d\omega'$ is a differential solid angle around direction Θ' $[sr]$,
- $L(x,\Theta)$ is the field radiance function $[W/(m^2 sr)]$,
- $\sigma(x)$ is the scattering coefficient $[1/m]$,
- $\kappa(x)$ is the extinction coefficient (often denoted by $k_t(x)$) $[1/m]$,
- $f(x,\Theta',\Theta)$ is the so-called phase function (often denoted by $P(x,\Theta',\Theta)$), which expresses the fraction of radiance radiated towards point x from direction Θ' that is scattered in direction Θ $[1/sr]$.

We do not consider emittance of media such as flames or plasma. The scattering may be anisotropic: $f(x,\Theta',\Theta)$ can be any function, as long as it is normalised over the

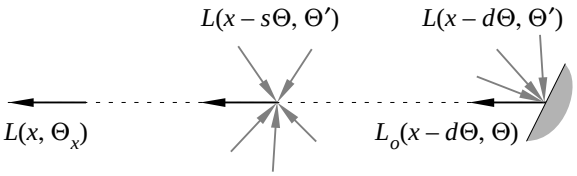

Fig. 1. The radiance equation expresses how light in a medium is the result of light inscattered along the line and light reflected from the surface.

sphere of directions and reciprocal. If we assume for a moment that the participating medium is homogeneous, i.e. $\kappa(x) = \kappa$ and $\sigma(x) = \sigma$, then the original integro-differential equation can be rewritten as the following integral equation (fig. 1):

$$L(x,\Theta) = \sigma \int_0^d \int_\Omega f(x - s\Theta, \Theta', \Theta) L(x - s\Theta, \Theta') d\omega'\, e^{-\kappa s} ds + L_o(x - d\Theta, \Theta) e^{-\kappa d} \tag{2}$$

where d is the distance to the nearest surface and $L_o(x - d\Theta, \Theta)$ is the outgoing radiance at that point. We can now also take into account the boundary conditions. The relation between incoming and outgoing radiance at surfaces is expressed by the well-known integral expression:

$$L_o(y,\Theta) = L_e(y,\Theta) + \int_{\Omega_i} f_r(y, \Theta', \Theta) L(y, \Theta') \, |\cos\theta'| \, d\omega' \tag{3}$$

where:

- $L_e(y,\Theta)$ is the self-emitted radiance at point x in direction Θ $[W/(m^2 sr)]$,
- $f_r(y,\Theta',\Theta)$ is the bidirectional reflectance distribution function (BRDF) $[1/sr]$,
- Ω_i is the hemisphere or sphere of incoming directions at point y,
- θ' is the angle between direction Θ' and the surface normal at point y.

Equations (2) and (3) define the behaviour of light in the medium and at surfaces respectively. Due to their integral formulations they are well-suited for Monte Carlo evaluation, which we will discuss in the next section.

3 Tracing a random walk

The sampling of the radiance equations is fairly straightforward and has been described for instance by Rushmeier [4]. It is intuitive in the sense that it can be regarded as a direct simulation of light particles scattering at dust or fog particles and reflecting at surfaces until they are absorbed. In this case a random walk starts from the eye point x, in a direction Θ pointing through a pixel. The radiance value $L(x,\Theta)$ can be estimated by performing a random walk. We can introduce a minor optimisation by first rewriting equation (2) as a single integral:

$$\begin{aligned} L(x,\Theta) &= \sigma \int_0^d \int_\Omega f(x - s\Theta, \Theta', \Theta) L(x - s\Theta, \Theta') d\omega'\, e^{-\kappa s} ds + L_o(x - d\Theta, \Theta) e^{-\kappa d} \\ &= \int_0^\infty \left[s < d \,?\, L_s(x - s\Theta, \Theta) : L_o(x - d\Theta, \Theta) \right] \kappa e^{-\kappa s} ds \end{aligned} \tag{4}$$

where $L_s(y, \Theta)$ is defined as:

$$L_s(y, \Theta) = \int_\Omega \frac{\sigma}{\kappa} f(y, \Theta', \Theta) L(y, \Theta') d\omega' \tag{5}$$

Equation (4) shows that the factor $\kappa e^{-\kappa s}$ can be used as a probability density function for the outer integral:

$$p_{medium}(s) = \kappa e^{-\kappa s} \tag{6}$$

From a physical point of view, this Poisson distribution expresses the probability density of a light particle interacting with the medium at distance s. If the nearest surface along the ray, at a distance d, lies further away than the point at distance s, the former term $L_s(x - s\Theta, \Theta)$ has to be estimated. Otherwise, the latter term $L_o(x - d\Theta, \Theta)$ has to be estimated. The ray tracing function, which determines the nearest surface, thus only has to look for surfaces within a distance s. For instance, in a foggy outdoor scene it is stochastically not always necessary to compute ray intersections with a village in the distance. The a posteriori probability of the light particle reaching the nearest surface is equal to the transmittance:

$$P_{surface}(d) = e^{-\kappa d} \tag{7}$$

Both terms $L_s(y, \Theta)$ and $L_o(y, \Theta)$ are estimated by sampling their respective integral expressions:

- $L_s(y, \Theta)$ is estimated by sampling the integral of equation (5) (fig. 2). A suitable subcritical PDF (i.e. it does not integrate to 1) for the scattered direction Θ' is:

$$p_{scattering}(\Theta') = \frac{\sigma}{\kappa} f(y, \Theta', \Theta) \tag{8}$$

- $L_o(y, \Theta)$ is expressed by equation (3). It consists of two terms. The self-emitted radiance $L_e(y, \Theta)$ can simply be evaluated. The second term is estimated by sampling the integral expression (fig. 3). A common subcritical PDF for the reflected direction Θ' is:

$$p_{reflection}(\Theta') = f_r(y, \Theta', \Theta) \, |\cos \theta'| \tag{9}$$

In both cases the radiance value $L(y, \Theta')$ is then estimated for the sampled direction. This recursive process results in a random walk through the scene. Because the latter PDFs are subcritical the random walk terminates with probability 1.

Stochastic ray tracing algorithms in general compute the direct illumination by explicitly sampling the light sources and tracing additional shadow rays, while the indirect illumination is computed as before. The process for generating random walks remains the same.

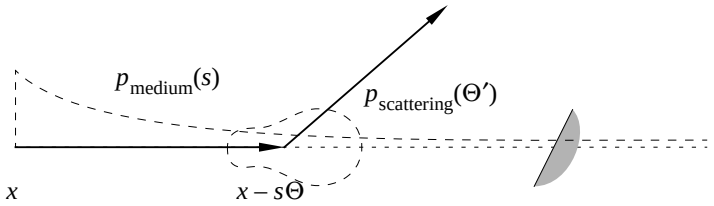

Fig. 2. Scattering on the random walk. First the distance s is sampled according to $p_{medium}(s)$, then the scattering direction Θ' according to $p_{scattering}(\Theta')$.

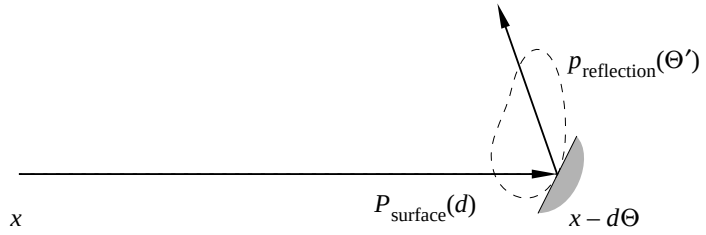

Fig. 3. Reflection on the random walk. If the distance s lies past the nearest surface, there is a reflection instead, with an a posteriori probability of $P_{surface}(d)$. In that case the reflection direction Θ' is sampled according to $p_{reflection}(\Theta')$.

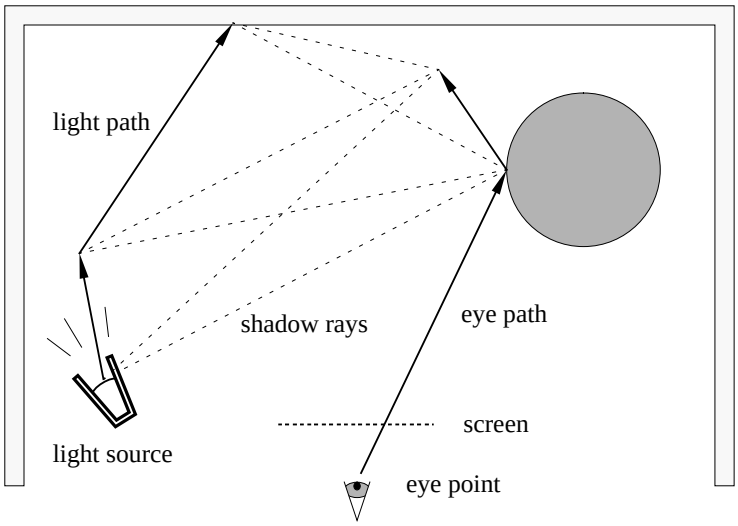

Fig. 4. A schematic overview of bidirectional path tracing in a participating medium. A pair of random walks is constructed: an eye path starting from the eye point, through a pixel, and a light path starting from a light source. The paths can scatter inside the medium or reflect at surfaces. The points on the respective paths are connected by means of shadow rays, which determine the contribution to the estimated flux of the pixel.

4 Bidirectional path tracing

Bidirectional path tracing has been introduced by us [14, 15] and has been presented independently and improved by Veach and Guibas [16, 17]. It combines the ideas of path tracing and light tracing by creating random walks, starting not only from the eye point, but also from the light sources. Figure 4 shows the basic idea. Eye paths start from the eye point, through the pixel that is being computed, as in classical path tracing. Light paths start from a sampled point on a light source in a sampled direction. Both types of random walks are generated as described in section 3. In the extension presented here, rays can be scattered or absorbed in the medium, as well as being reflected or absorbed at the surfaces of the scene.

After tracing a pair of random walks, the intersection points on the respective paths are connected by means of shadow rays. Each shadow ray that is not intercepted by an object in the scene contributes to the estimated flux or average radiance through the pixel.

The algorithm has proven to be particularly effective for rendering scenes with indirect illumination, compared to ordinary path tracing [18]. The different illumination transport paths present different estimators for the flux, each one with its own potential strength. A judicious combination of the estimators [17] yields a robust estimator with a generally lower variance. For this purpose the alternative estimators for illumination transport with the same number of reflections have to be considered in the same parameter space, for instance as the sequence of points $x_0, \ldots, x_k, y_l, \ldots, y_{-1}$ in the 3D space. The section $x_0 \to \ldots \to x_k$ is part of the light path, starting from a light source at point x_0. The section $y_l \leftarrow \ldots \leftarrow y_{-1}$ is part of the eye path, starting from the eye point y_{-1}.

The **illumination contribution** of the transport path in this parameter space is:

$$C_{kl}(x_0, \ldots, y_{-1}) = L_e(x_0 \to x_1)\,|\cos\theta_0| \times \frac{e^{-\kappa\|x_0 - x_1\|}}{\|x_0 - x_1\|^2} \times g(x_0 \to x_1 \to x_2) \times \frac{e^{-\kappa\|x_1 - x_2\|}}{\|x_1 - x_2\|^2} \times \ldots \times g(y_1 \to y_0 \to y_{-1}) \times \frac{e^{-\kappa\|y_0 - y_{-1}\|}}{\|y_0 - y_{-1}\|^2} \tag{10}$$

where we use the arrow notation for convenience. $\|x - y\|$ is the Euclidean distance between point x and point y. The function $g(x \to y \to z)$ accounts for the scattering or the reflection at point y on the random walk:

$$g(x \to y \to z) = \begin{cases} f(x \to y \to z) & \text{if the interaction is scattering,} \\ f_r(x \to y \to z)\,|\cos\theta_i|\,|\cos\theta_i'| & \text{if the interaction is reflection.} \end{cases}$$

where θ_i and θ_i' are the angles of the incoming and outgoing directions with the normal at point y.

The **probability density** for generating this path with the aforementioned eye path $x_0 \to \ldots \to x_k$ and light path $y_{-1} \to \ldots \to y_l$ is the product of their corresponding probability densities, as the random walks are independent:

$$p_{kl}(x_0, \ldots, y_{-1}) = p(x_0 \to \ldots \to x_k)\, p(y_{-1} \to \ldots \to y_l) \tag{11}$$

These probability densities in turn can be defined recursively:

$$p(x_0 \to \ldots \to x_i) = p(x_0 \to \ldots \to x_{i-1})\, p(x_i | x_0, \ldots, x_{i-1}) \tag{12}$$

where $p(X|Y)$ is the probability density for X if Y is known. The initial probability densities $p(x_0)$, $p(x_0 \to x_1)$, $p(y_{-1})$ and $p(y_{-1} \to y_0)$ depend on the sampling strategies for the pixel and the light sources respectively. The other probability densities are a function of the PDFs used for constructing the random walk, as presented in section 3. They depend on the types of interaction at points x_{i-1} and x_i:

$$p(x_i|x_0, \ldots, x_{i-1}) = \frac{p'(x_i)p''(x_i)}{\|x_i - x_{i-1}\|^2} \tag{13}$$

with

$$p'(x_i) = \begin{cases} p_{scattering}(x_{i-1} \to x_i) & \text{if the interaction at point } x_{i-1} \text{ is scattering,} \\ p_{reflection}(x_{i-1} \to x_i) & \text{if the interaction at point } x_{i-1} \text{ is reflection,} \end{cases}$$

and

$$p''(x_i) = \begin{cases} p_{medium}(\|x_{i-1} - x_i\|) & \text{if the interaction at point } x_i \text{ is scattering,} \\ P_{surface}(\|x_{i-1} - x_i\|) & \text{if the interaction at point } x_i \text{ is reflection.} \end{cases}$$

Together with the appropriate probability densities (11), the illumination contribution (10) can be combined into an unbiased estimator, as discussed in [17]. We have applied the balance heuristic, for which the weights of the illumination contribution can be written as follows:

$$w_{kl}(x_0, \ldots, x_k, y_l, \ldots, y_{-1}) = \frac{p_{kl}(x_0, \ldots, x_k, y_l, \ldots, y_{-1})}{\sum_i p_{k+i,l-i}(x_0, \ldots, x_k, y_l, \ldots, y_{-1})} \tag{14}$$

where the summation is over all possible types of transport paths for which contributions are added.

5 Extension to non-homogeneous media

While the previous sections only discuss homogeneous participating media, extension to non-homogeneous media is fairly straightforward. A common approach is to discretise the medium into volume elements, each having its own scattering characteristics. This representation particularly suits zonal methods and other techniques that already discretise the scene to compute the illumination. In a ray tracing context the discretisation can be traversed while tracing a ray, treating each element as a homogeneous medium, e.g. [13]. An alternative and slightly more general representation allows any function to describe the scattering characteristics of the medium. Typically, this is an empirical noise function that mimics media such as smoke plumes and clouds of dust.

We have opted for the latter approach, additionally bounding the participating media in the scene by means of simple volumes. For each ray piercing a volume with a participating medium the section of its traversal is determined. This section is then traversed at discrete intervals where the optical characteristics of the medium are sampled. Using this information a possible scattering can be sampled or the opacity can be estimated for each interval, in which the medium is approximated as homogeneous. The handling of non-homogeneous media thus becomes similar to the handling of homogeneous media. The traversal obviously requires additional work, depending on the coarseness of the discrete steps.

6 Implementation and results

We have implemented the presented extension in an existing bidirectional path tracing program. The scattering characteristics of the medium are modelled using the phase function proposed by Schlick [19], which is energy-conserving and reciprocal, and which is computationally inexpensive to evaluate and to use as a PDF.

Figure 5 shows a test scene with a few geometric objects with various optical characteristics. In image (b) the scene is engulfed in a slightly anisotropic cloud of smoke. It has been rendered at 640×480 pixels, with 100 samples per pixel. The bidirectional path tracing algorithm correctly renders the brightly lit lobe below the light source and the indirect illumination resulting from it. The combination of objects and the participating medium is smooth.

Figure 6 shows a church interior. The sun casts a beam of light through the stained-glass window, which is only visible in the dusty atmosphere in image (b). The sun is modelled as a spot light source outside. The stained-glass window is a translucent surface, scattering the incident light partly diffusely and partly directionally. The illumination of the interior is entirely indirect as a result. Classical path tracing would be very inefficient at rendering this scene. Only random walks that reach the outside would get an illumination contribution, resulting in a high variance. Bidirectional path tracing traces light paths to the inside, scattering and reflecting and eventually meeting the eye paths there.

Figure 7 illustrates the possible use of bidirectional path tracing for determining visibility in traffic scenes. In this case the algorithm also simulates the reflection and focusing of light by the reflectors of the headlights. In image (b) most of the car is illuminated indirectly by light that is scattered in the fog. Rendering more complex environments with traffic lights, traffic signs, puddles of water, etc. would be straightforward.

Figure 8 shows an interior scene with a fireplace, demonstrating the rendering of a non-homogeneous participating medium. The smoke rising from the fireplace is illuminated from below. It thus participates in the illumination of the rest of the room.

7 Conclusions

We have discussed the extension of bidirectional path tracing to include the effects of participating media in the simulation. The resulting algorithm correctly handles multiple scattering in non-emitting, non-homogeneous, anisotropic media. It provides unbiased estimators that are guaranteed to converge to the exact solution. Like most image-based Monte Carlo approaches, the algorithm is versatile and requires little memory. It is therefore well suited to render scenes with a combination of participating media and complex geometries and optical characteristics.

The required computation times may be taxing, however, even for the most hardened Monte Carlo user. The example images took several hours to render, with the computations distributed over some workstations. The presence of participating media markedly increases the complexity of the problem. Finite volume element techniques are not as flexible, but they are undoubtedly faster and more effective for simple scenes. Compared to unidirectional Monte Carlo approaches, the bidirectional algorithm presents a significant improvement. It handles scenes that were not tractable with classical path tracing. It also offers a solution for the light tracing approaches used in some visibility studies with participating media, by not requiring the artificially large detectors for receiving at least some light particles within a reasonable amount of time.

a) 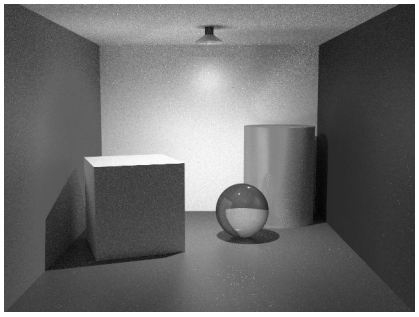 b) 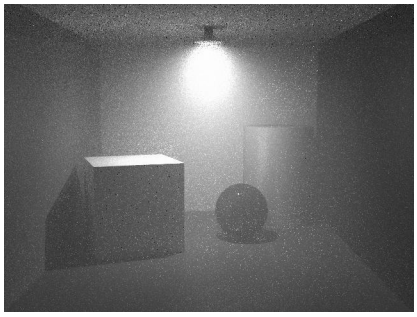

Fig. 5. Test scene: (a) without participating media, (b) with a dusty atmosphere.

a) 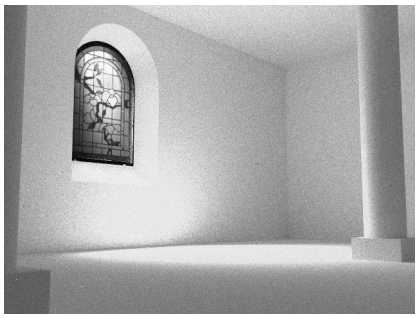 b) 

Fig. 6. Church interior: (a) without participating media, (b) with a dusty atmosphere.

a) 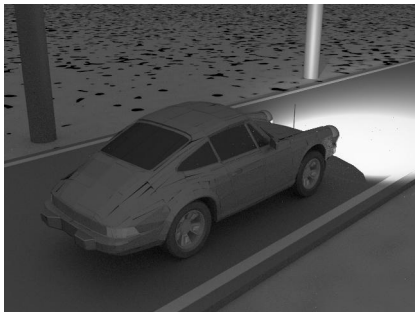 b) 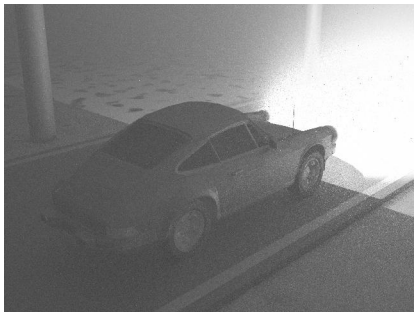

Fig. 7. Traffic scene: (a) without participating media, (b) with a foggy atmosphere.

Fig. 8. Fireplace scene with a non-homogeneous participating medium.

References

1. H. Rushmeier, "Rendering participating media: Problems and solutions from application areas," in *Proceedings of the Fifth Eurographics Workshop on Rendering*, (Darmstadt, Germany), pp. 35–55, June 1994.
2. E. Languénou, K. Bouatouch, and M. Chelle, "Global illumination in presence of participating media with general properties," in *Proceedings of the Fifth Eurographics Workshop on Rendering*, (Darmstadt, Germany), pp. 69–85, June 1994.
3. N. Max, "Efficient light propagation for multiple anisotropic volume scattering," in *Proceedings of the Fifth Eurographics Workshop on Rendering*, (Darmstadt, Germany), pp. 87–104, June 1994.
4. H. Rushmeier, *Realistic Image Synthesis for Scenes with Radiatively Participating Media*. PhD thesis, The Sibley School of Mechanical and Aerospace Engineering, Cornell University, 1988.
5. J. Kajiya and V. Herzen, "Ray tracing volume densities," *Computer Graphics*, vol. 18, pp. 165–174, July 1984.
6. J. Stam, "Multiple scattering as a diffusion process," in *Proceedings of the Sixth Eurographics Workshop on Rendering*, (Dublin, Ireland), pp. 69–79, June 1995.
7. Ch. Patmore, "Simulated multiple scattering for cloud rendering," in *Proceedings of ICCG*, (Bombay, India), pp. 59–70, Feb. 1993.
8. N. Bhate and A. Tokuta, "Photorealistic volume rendering of media with directional scattering," in *Proceedings of the Third Eurographics Workshop on Rendering*, (Bristol, UK), pp. 227–245, May 1992.
9. J. Kajiya, "The rendering equation," *Computer Graphics*, vol. 20, pp. 143–150, Aug. 1986.
10. J. Arvo, "Backward ray tracing," Aug. 1986.
11. B. Roysam, A. Cohen, P. Getto, and P. Boyce, "A numerical approach to the computation of light propagation through turbid media: Application to the evaluation of lighted exit signs," *IEEE Transactions on Industry Applications*, pp. 661–669, May 1993.
12. C. Rozé, B. Maheu, and G. Gréhan, "Evaluations of the sighting distance in a foggy atmosphere by Monte Carlo simulation," *Atmospheric Environment*, vol. 28, no. 5, pp. 769–775, 1994.
13. S. Pattanaik, *Computational Methods for Global Illumination and Visualisation of Complex 3D Environments*. PhD thesis, NCST Birla Institute of Technology & Science, Pilani, India, Feb. 1993.
14. E. Lafortune and Y. Willems, "Bi-directional path tracing," in *Proceedings of CompuGraphics*, (Alvor, Portugal), pp. 145–153, Dec. 1993.
15. E. Lafortune and Y. Willems, "A theoretical framework for physically based rendering," *Computer Graphics Forum*, vol. 13, pp. 97–107, June 1994.
16. E. Veach and L. Guibas, "Bidirectional estimators for light transport," in *Proceedings of the Fifth Eurographics Workshop on Rendering*, (Darmstadt, Germany), pp. 147–162, June 1994.
17. E. Veach and L. Guibas, "Optimally combining sampling techniques for Monte Carlo rendering," *Computer Graphics*, vol. 29, pp. 419–428, Aug. 1995.
18. E. Lafortune, *Mathematical Models and Monte Carlo Algorithms for Physically Based Rendering*. PhD thesis, Katholieke Universiteit Leuven, Belgium, Feb. 1996.
19. Ch. Schlick, *Divers Eléments pour une Synthèse d'Images Réalistes*. PhD thesis, Université Bordeaux 1, France, Nov. 1992.